

Binary and Multiclass Leukemia Classification Using a Hybrid Deep Learning-ML Approach: Towards an Explainable AI Framework

Amit Sharma
Professor , School of Computer Applications Lovely Professional University, Phagwara, Punjab, India.
profamitsharma@gmail.com

K. Ranjith Singh
Department of Computer Science Karpagam Academy of Higher Education Coimbatore- 641021
ranjithsingh.k.kahe@kahedu.edu.in

Rahul Gupta
Adjunct Faculty, School of Management - PG Management JAIN (Deemed to be University), Bangalore, Karnataka
rahul_g@cms.ac.in

Raman Verma,
Centre of Research Impact and Outcome, Chitkara University, Rajpura-140417, Punjab, India
raman.verma.orp@chitkara.edu.in

Deepika Dongre,
Assistant Professor, AI & DS, Vishwakarma Institute of Technology , Pune , India,
deepika.dongre@viit.ac.in

Prateek Garg,
Chitkara Centre for Research and Development, Chitkara University, Himachal Pradesh-174103 India
prateek.garg.orp@chitkara.edu.in

Abstract— Within the latter phases of the disease, the spreading of leukaemia in people generates a great deal of concern. Blood production in the bone marrow is hindered as a result of this. For the purpose of diagnosis in this instance, morphology analysis of blood cells from people is a method that is well-known and has been well tested. Both normal cells and cells that have been infected with leukaemia may be differentiated using the binary categorization. In addition, the therapy for various types of leukaemia is distinct from one another. For a correct diagnosis of the kind of leukaemia, it is also necessary to identify these subclasses. The determination of the leukaemia subtype requires the use of multiple classifications. Microscopical inspection of these blood cells is often used to accomplish this task. A further reason why the procedure for making choices is so important is that it necessitates the presence of a skilled pathology. This led to the creation of a software-based structure for diagnosis. The investigators used methods of machine learning that are considered to be state-of-the-art. These methods include support vector machine (SVM), random forest (RF), naïve bays, k-nearest neighbour (KNN), and others. However, these methods result in the accuracy of classification that is restricted. Researchers also make use of more sophisticated varieties of deep learning techniques. The suggested XGBoost approach outperformed all models with 97% accuracy. DenseNet-XGBoost and Xception-RF performed well, but Inception-ResNet and Random Forest(RF) performed moderately. ResNet-RF was lowest. Thus, the suggested leukemia categorization method works best.

Keywords- Xception-RF, XGBoost, ResNet-RF, DenseNet-XGBoost, Inception-ResNet, leukaemia, XGBoost.

I. INTRODUCTION

The malignancy that affects the bone marrow and the blood is of this sort. After beginning in the cells of the bone marrow that are responsible for producing blood, it eventually makes its way into the circulation. In the long run, the illness will inevitably spread to other areas of the body [1]. When

leukaemia is categorized as chronic, it often signifies that the disease is sluggish to spread and increases in severity. On the contrary hand, chronic myelogenous leukaemia (CML) may gradually develop into an acute type of leukaemia that is quickly developing and has the potential for spread to almost each organ in the body. The ability of the bone marrow to produce blood is often something that is affected by leukaemia. A bones marrow cell is the starting point for leukaemia. The cell undergoes a transformation and transforms into a leukaemia cell type. Following the transformation of the bone marrow cell into a leukemic cell, leukaemia cells may be able to multiply and survive more effectively than normal cells. Over the course of time, patients with leukaemia either crowd out or repress the formation of normal cells.

A varied pace of development and a distinct manner in which the cells replace typical blood and bone marrow cells are characteristic of each form of leukaemia [2]. One of the symptoms of leukaemia is a spike in the total amount of blast cells, which is caused by a viral infection in the blood. The blasts in question are young WBCs. Considering the larger number of explosions there is a very limited amount of room for red blood cells to go throughout the bloodstream. As a consequence of this, the proportion of red blood cells (RBC) declines, which leads to anaemia as well as other problems. Chronic and acute leukaemia's, as well as lymphoblastic and myeloid leukaemia's, are the two categories that make up leukaemia categories.

The build-up of abnormal white blood cells (leukaemia cells) in the marrow of the bones causes acute lymphoblastic leukaemia, also called acute lymphoid leukaemia, a kind of blood cancer [3-5]. Rapid cell death caused by ALL occurs when normal, maturing cells are supplanted by abnormal, immature leukaemia cells.



Normal Blood



Leukemia

Fig 1: Normal and leukemic cells

The lymph nodes of the brain, the liver, and the testes are among the structures of the body where leukaemia cells may invade and multiply in the circulation. Multiple signs may be caused by the growth, division, and spread of these cancer cells [6-7]. A greater number of B lymphocytes compared to T lymphocytes is usually seen in ALL. Preventing the body from harmful bacteria and diseases and eliminating diseased cells are important functions of B and T cells. Specifically, B cells assist in avoiding germ infections, whereas T cells kill off infected cells.

This rapidly expanding malignancy of the bloodstream and bone marrow goes by many names: acute myelogenous leukaemia, acute myeloblastic leukaemia, acute granulocytic leukaemia, and acute nonlymphocytic leukaemia [8]. The AML subtype is the most prevalent form of acute leukaemia. The production of immature cells called blasts by the bone marrow triggers this process. As is typical, these blasts differentiate into WBCs.

II. RELATED WORKS

Researchers employ a variety of techniques to identify leukemia, including support vector machines (SVM), k-means clustering, K-nearest neighbors (K-NN), naive Bayes, the Zack algorithm, and deep learning methods such as CNN, deep learning nets, CNN plus SVM strategy, AlexNet, and SVM classifiers. In this particular study, two characteristics, geometry and local binary pattern (LBP), yielded accuracy rates of 89.72% and 88.79%, respectively [9-10].

Table 1 : Summary of the state of the Art work in the Similar Field.

Methodology	Advantages	Limitations
SIFT, SURF, ORB feature extraction, SNV, KNN, RF classifiers [11]	Achieved 94.3% accuracy using RF	Needs categorization and preliminary processing; characteristics are restricted to those that have

		been hand-crafted.
Ensemble classifier, morphological and textural features [12-13]	Accuracy of 94.73% using ensemble classifier	Not suitable for use with real-world images; just takes binary categorization into account.
GLCM feature extractor, probabilistic PCA, RF classifier [14-16]	Utilizing marker-based classification to enhance property extraction	The method of segmentation is laborious, and it is only possible to do binary classification (ALL vs. Normal). .
GLRLM and GLCM texture features, PCA, SVM classifier [17-19]	Characteristics of texture, color, and form integrated for enhanced performance	With big datasets, sub-image segment may not work very well; it's also only good for binary categorization. .

The author utilized a method founded on CNNs to identify white blood cells in photographs of blood taken under a microscope. Here, we merge the characteristics of the top and bottom layers to boost efficiency [20-24]. This method used CNN for removing features after preliminary processing and segmented. Considering the real-image collection is essential for generalizing this strategy.

III. PROPOSED METHODOLOGY

Illustrates the suggested hybrid strategy technique for diagnosing leukaemia utilizing multi-class & binary classifications. Later on, the dataset's pictures will be analysed and spread for categorization. The ALL-IDB database is used for the procedure. Multiple frameworks make use of convolutional neural networks to solve problems. Notable frameworks including DenseNet, InceptionResNet, Xception, and ResNet are utilized for the extraction of features.

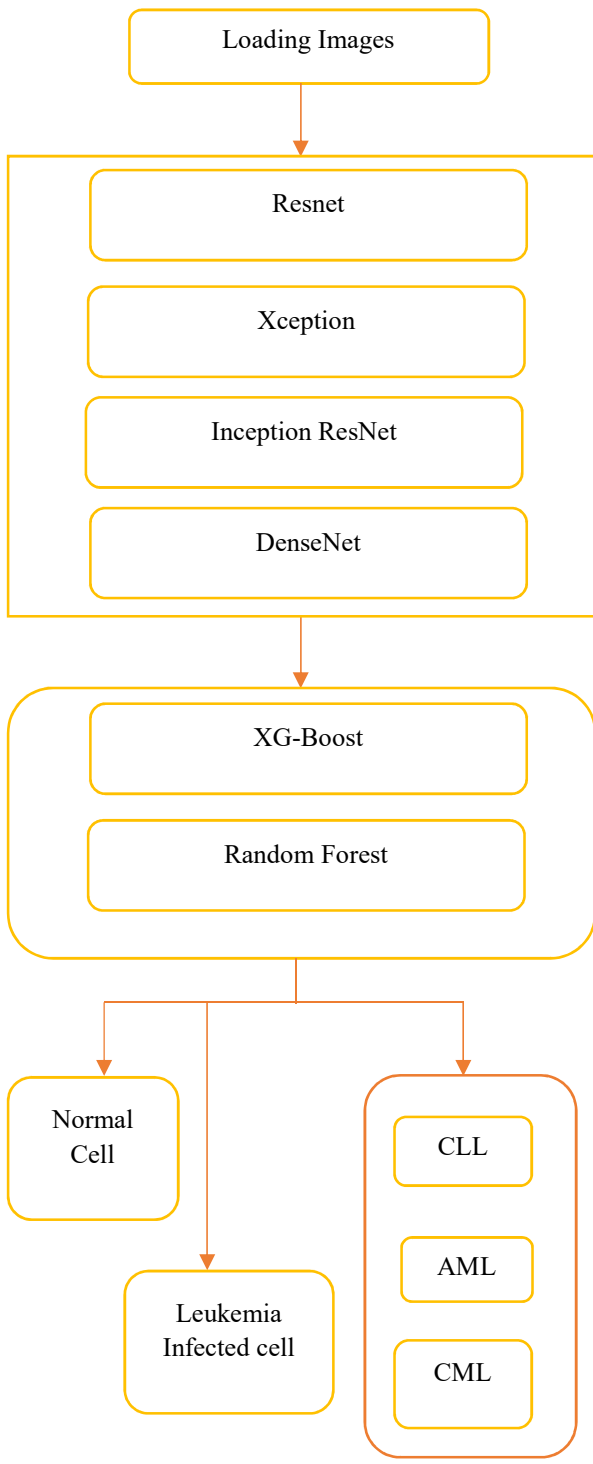


Fig 2 : Approach of classifying leukaemia

3.1 Resnet:

Model variation reset. A total of fifty layers makes it up. One typical pooling layer and forty-eight layers of convolution make up the model. It has one layer of convolution that uses 64 separate kernels with a size of 7x7. Layers are all stride at 2. A maximum pooling level with a stride 2 size follows that. Once again, we have a convolutional with an 11-layer structure with 64 kernels, followed by a 33-sized kernel, and so on, up to a 64-layer structure with 256 kernels. This stage contains nine levels. Next to it is a kernel of 11, 128. Next,

there is going to be a 33.122-sized kernel and, in the last step, an 11.1-sized kernel. Four iterations of this process resulted in twelve layers.

3.2 Xception :

The depth wise convolutions to the in this are separable. The "extreme" variant of an Inception module is called Xception. "Xception" stands for "extreme inception" and refers to the application of the Inception concepts. We used several filters on every level of space derived from those inputs areas, and Inception utilized 1x1 convolutions to reduce the initial input. Xception immediately turns this process backwards. In a neural networks architecture, this approach is quite similar to depth-wise separated convolution. There is yet another difference between Xception and Inception.

3.3 Inception ResNet:

Training for Inception-ResNet-v2 was carried out on a vast imagery dataset. During this training, the database of ImageNet was used. One of the many uses for the 164-layer network is object classification. Hence, the neural network has picked up very accurate representations of characteristics for many different kinds of pictures. As input, the network takes in a 299 x 299 picture and produces predicted probability of classes. To put it simply, it combines elements from both Inception and remaining relationships. With a convolution filter that combines different sizes, it has a residue connection. By using residual connections, the decrease in performance problem is mitigated, and the training time is shortened with some success.

3.4 DenseNet:

It trains more efficiently because relationships between its layers are shorter. Deeper connections exist between all of the levels here. Data may move easily all through the system according to the design in Figure 2. A feed-forward feature is maintained by having information from earlier levels passed on to each subsequent layer. Next, map features are used to transmit the same data to the layers that follow. Multiple layers' worth of characteristics are combined. Therefore, those feature mappings from the preceding convolution blocks make up the i th layer, which has I input. Each successive ' $I-i$ ' layer receives its own map of features. This architecture uses ' $(I(I+1))/2$ ' links in the network, which is different from standard deep learning designs. It uses fewer variables than regular CNN because it skips learning irrelevant feature maps. The two most crucial parts of DenseNet are the pooling and primary convolutional layering. Dense Block and Transitional Layer are the names of these. Classifier using well-known, state-of-the-art classical ML techniques follows the extraction of characteristics. Deep learning systems use XGBoost and random-forest classifier after the extraction of features.

3.5 XG-Boost:

"XGBoost (Extreme Gradient Boosting) is a distributed gradient-boosted decision tree (GBDT) machine learning library." Identification, regression, however, and ranking are just a few of the many challenges it can handle. You may use

this approach with boosting parallel trees without any problems. In many instances, XGBoost's implementation of Gradient Boosted decision trees proves to be successful. This program builds decision trees in a sequential fashion. In XGBoost, weights show a noteworthy role. All of the method's variables that are autonomous have weights given to them. The decision tree usages those bulks to make a forecast. We feed the factors that the first decision tree got wrong into the second one and give them more weight. The next step is to merge each of the classifications and predictions into a single, stronger model. Issues with ranking, categorization, regression, and defined by users predictions are all under its purview.

$$j(0) = \sum_{i=1}^m M(x_i, x_i) + \sum_{l=1}^L (e_l) \quad (1)$$

The loss functional between the real label x_i and anticipated label x_i is represented by $M(x_i, x_i)$. (e_l) = The complexity-controlling normalization parameter for the (l) -tree.

The standard definition for a quadratic function of loss is:

$$M(x, x) = \frac{1}{2} \sum_{i=1}^m (x_i - x_i)^2 \quad (2)$$

In order to change weights, XGBoost employs the second-degree approximations of the loss feature:

$$f_i = \frac{\partial M(x_i, x_i)}{\partial x_i} \quad (3)$$

$$j_i = \frac{\partial^2 M(x_i, x_i)}{\partial x_i^2} \quad (4)$$

Where: f_i = the loss of the function's initial derivatives (gradient). The second derivatives (Hessian) of a loss function is equal to j_i .

$$x_i = -\frac{\sum_{i \in I_j} f_i}{\sum_{i \in I_j} v_i} \quad (5)$$

Every occurrence in leaf a is part of the set I_j .

3.6 Random Forest:

The prediction of output is accomplished by these models by the accumulation of the outcomes of many regresses' decision trees. Numerous decision trees are included in it, each of which has its own individual collection of data for training. In the end, our approach performs much better in solving classification problems when contrasted with a decision tree. The technique of pruning and the branching criterion are considered to be the two most essential topics as of right now. The selection of this approach is based on the amount of trees that are generated as well as the samples that are used by every node. It is important to note that the tree allocation in the forest does not change, since each tree is created individually as a vector that has been randomly

sampled depending on the input data. By using bootstrap clustering and random selection of features, the forest projections get averaged out.

$$H(R, B) = \sum_{i=1}^n x_i H_s(R_i) \quad (6)$$

R represents the data set that was divided at the node. B is characteristic that is being divided up. The "impurity" measurement for the subset, such as the Gini index or the entropy is denoted as (R_i) . The weights for every split, denoted by R_i , is equal to X_i .

$$H(R) = 1 - \sum_{l=1}^L q_l^2 \quad (7)$$

L is the number of courses. The probability of selecting category l from the collection S is denoted as q_l .

$$x = \frac{1}{m} \sum_{i=1}^m U_l(y) \quad (8)$$

The output of the i -th decision tree for the input variable y is represented by $U_i(y)$.

IV. RESULT

The disease that may become fatal in its advanced stages is leukaemia in extreme cases. The therapeutic suggestions differ for each of its subtypes. Therefore, the multiclass categorization of cells with leukaemia into several subtypes served as the basis for the current investigation. The system was further tested for the purpose of subtype leukaemia predictions using a real-image collection consisting of pictures classified as AML, CML, or CLL. Here, a DL-ML architecture is proposed as a foundation for the hybrid approaches. To gather attributes, the transfer technique for learning employs well-known deep neural network algorithms.

4.1. Accuracy: The true positive and true negative rates are expressed as a percentage of the total cases. It shows the percentage of correct predictions relative to the total number of data.

4.2. Precision: The ratio of actual positive results to the total number of positive predictions is known as precision. It shows that a lot of the optimistic forecasts came true.

4.3. Recall: Recall quantifies the ratio of true positives to actual positives, also known as sensitive. The model catches all positive situations effectively.

4.4. F1-Score: F1-Score is precision-recall harmonics average. Especially effective with skewed datasets, it balances accuracy and recall to provide a single model performance indicator.

Table 2: Evaluations of performance demonstrating several feature extractors

Methods	Accuracy	Precision
ResNet -RF	0.76	0.76
Xception -RF	0.92	0.95
Inception ResNet - XGBoost	0.87	0.83
DenseNet - XGBoost	0.96	0.92
RF	0.89	0.87
XGBoost	0.97	0.96

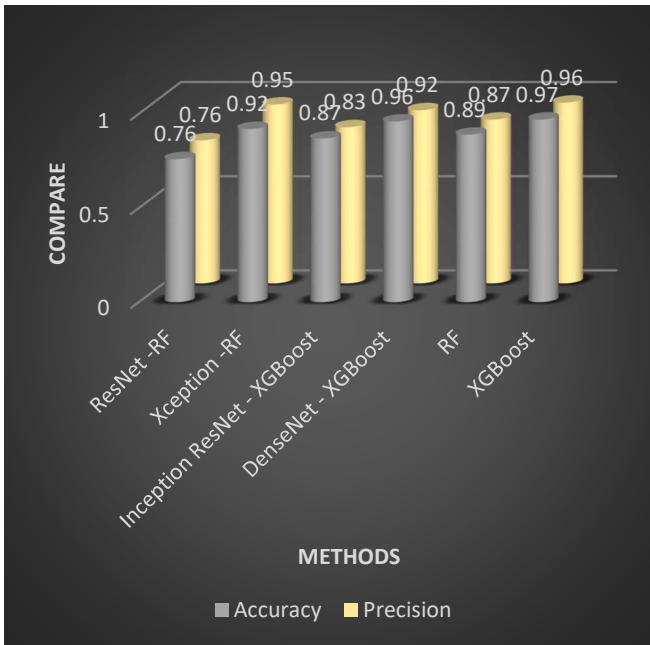


Fig 3: Efficiency of different methods

The table compares the precision and accuracy measurements of different approaches. With a success rate of 0.97 and precise of 0.96, the XGBoost model classifies leukemia subtypes best. The DenseNet-XGBoost combo follows with 0.96 accuracy and 0.92 precision, showing the power of ensembles training and deeper extraction of features. Having an accuracy of 0.92 and a precision of 0.95, the Xception-RF model shows the feature extractor's efficacy. In contrast, Inception ResNet-XGBoost and RF models performed moderately with accuracy ratings of 0.87 and 0.89, accordingly, while ResNet-RF trails behind at 0.76, indicating weaker generalization capabilities. Overall, XGBoost-based systems outperformed Random Forest-based algorithms because to its ability to manage complicated data interactions.

Table 3: Analysing the Potential of the proposed Approaches

Methods	Recall	F1 - Score
---------	--------	------------

ResNet -RF	0.77	0.78
Xception -RF	0.86	0.88
Inception ResNet - XGBoost	0.76	0.84
DenseNet - XGBoost	0.89	0.81
RF	0.91	0.89
XGBoost	0.96	0.95

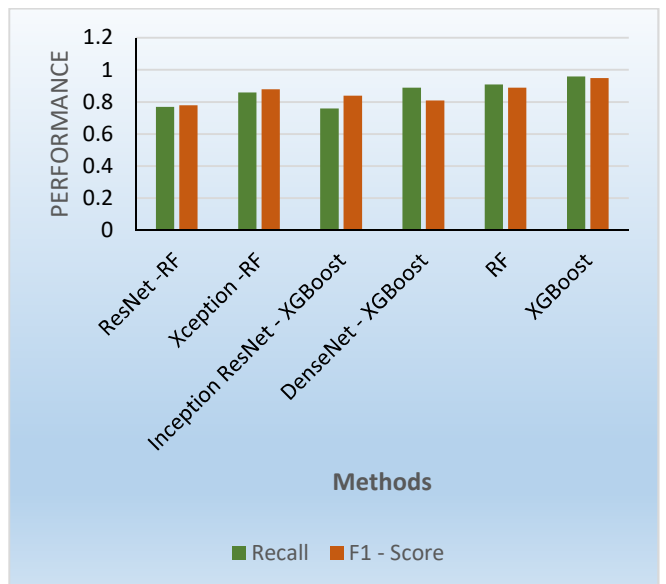


Fig 4: Comparison of different models

The XGBoost technique outstripped the other algorithms in terms of recall (0.96) and F1-score (0.95), demonstrating its exceptional sensitivity-to-precision balancing. With an F1-score of 0.89 and a recall of 0.91, the technique known as Random Forest also did rather well. Xception-RF was not as effective as the best approaches, but it still performed well with a recall of 0.86 and an F1-score of 0.88. DenseNet-XGBoost's recall was strong at 0.89 but its F1-score was low at 0.81, indicating a discrepancy between the two metrics. Both ResNet-RF (0.77 recall, 0.78 F1-score) and Inception ResNet-XGBoost (0.76 recall, 0.84 F1-score) were the least successful in collecting true positives, according to the results. When comparing recall and F1-score, XGBoost was clearly the best approach.

V. CONCLUSION

The categorization and treatment of leukemia are carried out using a hybrid DL-ML paradigm. There are two approaches to categorization. The outcome of this binary categorization is an indication of whether the cells are healthy or contaminated. Another method makes use of a real-world picture collection to do multi-class categorization. Leukemia may be further classified into three subtypes: AML, CML, and CLL. When it comes to categorization, deep learning consistently outperforms machine learning. In terms of

leukemia diagnosis, the quantity of the dataset is the primary limitation. Consequently, a mix of deep learning and machine learning is used for categorization in a hybrid method. Xception, InceptionResV2, DenseNet, and ResNet are among the frameworks used to extract characteristics, together with deep learning classifiers and convolution neural networks. The most cutting-edge artificial intelligence classifiers is used to accomplish the final categorization. When it comes to categorization, XGBoost and Random-forest are both being examined. The leukemia diagnostic performance is enhanced by the suggested method. In the present investigate, the testing accuracy levels were close to 100% for the ALL-IDB dataset and 97% for the actual picture dataset. It is necessary to go deeper into the same classification process for different kinds of leukaemia.

REFERENCES

- [1] N. M. Deshpande, S. Gite, R. Aluvalu, " A review of microscopic analysis of blood cells for disease detection with AI perspective". PeerJ Computer Science, 7, e460. <https://doi.org/10.7717/peerj-cs.460.7> , (2021).
- [2] N. Malik, "Authentic leadership – an antecedent for contextual performance of Indian nurses," Personnel Review, vol. 47, no. 6, pp. 1244–1260, Sep. 2018, doi: <https://doi.org/10.1108/pr-07-2016-0168>.
- [3] S. Kala, H. Nandan, and P. Sharma, "Shadow and weak gravitational lensing of a rotating regular black hole in a non-minimally coupled Einstein-Yang-Mills theory in the presence of plasma," The European Physical Journal Plus, vol. 137, no. 4, Apr. 2022, doi: <https://doi.org/10.1140/epjp/s13360-022-02634-6>.
- [4] K. Sood, M. Dev, K. Singh, Y. Singh, and D. Barak, "Identification of Asymmetric DDoS Attacks at Layer 7 with Idle Hyperlink," ECS Transactions, vol. 107, no. 1, pp. 2171–2181, Apr. 2022, doi: <https://doi.org/10.1149/10701.2171ecst>.
- [5] C. Prabhu, R. V. Gandhi, A. K. Jain, V. S. Lalka, Sree Ganesh Thottappudi, and P. P. Rao, "A Novel Approach to Extend KM Models with Object Knowledge Model (OKM) and Kafka for Big Data and Semantic Web with Greater Semantics," Advances in intelligent systems and computing, pp. 544–554, Jun. 2019, doi: https://doi.org/10.1007/978-3-030-22354-0_48.
- [6] V. Roy and S. Shukla, "Image Denoising by Data Adaptive and Non-Data Adaptive Transform Domain Denoising Method Using EEG Signal," in Proceedings of All India Seminar on Biomedical Engineering 2012 (AISOBEC 2012), V. Kumar and M. Bhatele (eds.), Lecture Notes in Bioengineering. Springer, India, 2013. https://doi.org/10.1007/978-81-322-0970-6_2.
- [7] V. Roy and S. Shukla, "A NLMS Based Approach for Artifacts Removal in Multichannel EEG Signals with ICA and Double Density Wavelet Transform," 2015 Fifth International Conference on Communication Systems and Network Technologies, 2015, pp. 461-466, doi: [10.1109/CSNT.2015.61](https://doi.org/10.1109/CSNT.2015.61).
- [8] Garg, S., Kaur, K., Kumar, N., & Rodrigues, J. J. P. C. (2019). Hybrid deep-learning-based anomaly detection scheme for suspicious flow detection in SDN: a social multimedia perspective. *IEEE Transactions on Multimedia*, 21(3), 566–578.
- [9] P. Kumar, A. Baliyan, K.R. Prasad, N. Sreekanth, P. Jawarkar, V. Roy, E.T. Amoatey, "Machine Learning Enabled Techniques for Protecting Wireless Sensor Networks by Estimating Attack Prevalence and Device Deployment Strategy for 5G Networks," *Wireless Communications and Mobile Computing*, vol. 2022, Article ID 5713092, pp. 1-15, 2022. <https://doi.org/10.1155/2022/5713092>.
- [10] H. Gupta and C. Sharma, "Face mask detection using transfer learning and OpenCV in live videos," 2022 International Conference on Fourth Industrial Revolution Based Technology and Practices (ICFIRTP), pp. 115–119, Nov. 2022, doi: <https://doi.org/10.1109/icfirtp56122.2022.10059441>.
- [11] V. Singh, R. Bansal, and R. B. Singh, "Big-Data Analytics," pp. 275–291, Oct. 2022, doi: <https://doi.org/10.1002/9781119792826.ch12>.
- [12] A. Kashyap and J. Raghuvanshi, "A preliminary study on exploring the critical success factors for developing COVID-19 preventive strategy with an economy centric approach," Management Research: Journal of the Iberoamerican Academy of Management, vol. 18, no. 4, pp. 357–377, Sep. 2020, doi: <https://doi.org/10.1108/mrjam-06-2020-1046>.
- [13] V. Roy, S. Shukla, "Enhanced Empirical Mode Decomposition Approach to Eliminate Motion artifacts in EEG using ICA and DWT" , International Journal of Signal Processing, Image Processing and Pattern Recognition , 2016, Vol. 9, No. 5, pp.321-338, DOI: [10.14257/ijspip.2016.9.5.29](https://doi.org/10.14257/ijspip.2016.9.5.29).
- [14] V. V. Bertero, "Observations of structural pounding," in Proceedings of the International Conference: The Mexico Earthquake–1985, Mexico City, Mexico, August 1986.
- [15] Y. N. Prajapati and M. Sharma, "Designing AI to Predict Covid-19 Outcomes by Gender," Dec. 2023, doi: <https://doi.org/10.1109/icdsai59313.2023.10452565>.
- [16] Y. N. Prajapati and M. Sharma, "Novel Machine Learning Algorithms for Predicting COVID-19 Clinical Outcomes with Gender Analysis," Communications in computer and information science, pp. 296–310, Jan. 2024, doi: https://doi.org/10.1007/978-3-031-56703-2_24.
- [17] S. S. Gupta, T. K. Pandey, V. P. Raju, R. Shrivastava, R. Pandey, A. Nigam, V. Roy, "Diabetes Estimation Through Data Mining Using Optimization, Clustering, and Secure Cloud Storage Strategies", SN Computer Science, (2024) 5(781), <https://doi.org/10.1007/s42979-024-03158-9>.
- [18] M. Alrizq, S. Stalin, S. Sultan, V. Roy, A. Mishra, A. Chandanan, N. Awadallah, P. Venkatesh, (2023). Optimization of sensor node location utilizing artificial intelligence for mobile wireless sensor network. *Wireless Networks*. 1-13. [10.1007/s11276-023-03469-4](https://doi.org/10.1007/s11276-023-03469-4).
- [19] J. A. Khan, R. S. Rathore, H. H. Abulreesh, A. S. Al-thubiani, S. Khan, and I. Ahmad, "Diversity of antibiotic-resistant Shiga toxin-producing Escherichia coli serogroups in foodstuffs of animal origin in northern India," Journal of Food Safety, vol. 38, no. 6, p. e12566, Oct. 2018, doi: <https://doi.org/10.1111/jfs.12566>.
- [20] S. Pathan, "Agricultural plant diseases identification: From traditional approach to deep learning," Materials Today: Proceedings, vol. 80, pp. 344–356, 2023. [Online]. Available: <https://doi.org/10.1016/j.matpr.2023.02.370>
- [21] D. Gade, "ICT based Smart Traffic Management System 'iSMART' for Smart Cities," International Journal of Recent Technology and Engineering, vol. 8, no. 3, pp. 3920–3928, Sep. 2019, doi: <https://doi.org/10.35940/ijrte.c5137.098319>.
- [22] G. Chauhan and V. Chauhan, "A phase-wise approach to implement lean manufacturing," International Journal of Lean Six Sigma, vol. 10, no. 1, pp. 106–122, Mar. 2019, doi: <https://doi.org/10.1108/ijlss-09-2017-0110>.
- [23] K. Ramu, S. V. S. R. K. Raju, S. Singh, V. Rachapudi, M. A. Mary, V. Roy, S. Joshi, "Deep Learning-Infused Hybrid Security Model for Energy Optimization and Enhanced Security in Wireless Sensor Networks", SN Computer Science, 5:848, 2024, <https://doi.org/10.1007/s42979-024-03193-6>.
- [24] Prabhat Kumar Srivastava, S. Kumar, A. Tiwari, D. Goyal, and Udit Mamodiya, "Internet of thing uses in materialistic ameliorate farming through AI," AIP Conference Proceedings, Jan. 2023, doi: <https://doi.org/10.1063/5.0154574>.